0026-895X/99/020300-08$3.00/0

MOLECULAR PHARMACOLOGY, **56:**300–307 (1999).

Identification of Amino Acids of the Torpedo Nicotinic Acetylcholine Receptor Contributing to the Binding Site for the Noncompetitive Antagonist [^{3}H]Tetracaine

MARTIN J. GALLAGHER[1] and JONATHAN B. COHEN

Department of Neurobiology, Harvard Medical School, Boston, Massachusetts

Received March 23, 1999; accepted May 18, 1999

This paper is available online at http://www.molpharm.org

ABSTRACT

[^{3}H]Tetracaine is a noncompetitive antagonist of the *Torpedo* nicotinic acetylcholine receptor (nAChR) that binds with high affinity in the absence of cholinergic agonist (K_{eq} = 0.5 μM) and weakly (K_{eq} = 30 μM) in the presence of agonist (i.e., to nAChR in the desensitized state). In the absence of agonist, irradiation at 302 nm of nAChR-rich membranes equilibrated with [^{3}H]tetracaine results in specific photoincorporation of [^{3}H]tetracaine into each nAChR subunit. In this report, we identify the amino acids of each nAChR subunit specifically photolabeled by [^{3}H]tetracaine that contribute to the high-affinity binding site. Subunits isolated from nAChR-rich membranes photolabeled with [^{3}H]tetracaine were subjected to enzymatic digestion, and peptides containing ^{3}H were purified by SDS-polyacrylamide gel electrophoresis followed by reversed phase HPLC. N-terminal sequence analysis of the isolated peptides demonstrated that [^{3}H]tetracaine specifically labeled two sets of homologous hydrophobic residues (αLeu^{251}, βLeu^{257}, γLeu^{260}, and δLeu^{265}; αVal^{255} and δVal^{269}) as well as αIle^{247} and δAla^{268} within the M2 hydrophobic segments of each subunit. The labeling of these residues establishes that the high-affinity [^{3}H]tetracaine-binding site is located within the lumen of the closed ion channel and provides a definition of the surface of the M2 helices facing the channel lumen.

The nicotinic acetylcholine receptor (nAChR) isolated from the electric organ of the marine ray *Torpedo* is the best characterized ligand-gated ion channel (for reviews, see Karlin and Akabas, 1995; Hucho et al., 1996). The nAChR is composed of four homologous subunits in the stoichiometry $\alpha_2\beta\gamma\delta$, which electron microscopic studies show are arranged pseudosymmetrically about a central axis that is the ion channel (Unwin, 1993). The M2 hydrophobic segments from each subunit line the lumen of the ion channel (Hucho et al., 1986; Imoto et al., 1988, 1991; Charnet et al., 1990; Revah et al., 1990) and undergo a conformational change when the nAChR binds agonist (White and Cohen, 1992; Akabas et al., 1994; Unwin, 1995). Within the M2 domain, a conserved leucine (αLeu^{251} and the homologous position in the other subunits) appears to be important for the gating of the ion channel. Cryoelectron microscopy reveals an agonist-dependent rotation of a kink in the M2 helices near the predicted position of these leucines (Unwin, 1995), referred to as position 9 with reference to the conserved Lys at the N-terminal end of each M2 segment, and site-directed mutagenesis demonstrates that this position is an important determinant of the equilibrium between closed and open channel states (Filatov and White, 1995; Labarca et al., 1995). However, it is unclear whether this ring of leucines forms the permeability barrier in the closed channel because cysteine mutants below position 9 are accessible to water-soluble sulfhydryl reagents in the absence of agonist (Akabas et al., 1994; Pascual and Karlin, 1998).

Noncompetitive antagonists (NCAs), which are compounds that block the permeability response without preventing the binding of agonist, have also been used to characterize the structure of the ion channel pore. For nAChR in the desensitized state, [^{3}H]chlorpromazine is photoincorporated into residues at position 6 of each subunit's M2 segment as well as into position 2 in βM2 and 9 in βM2 and γM2 (Giraudat et al., 1986, 1987, 1989; Revah et al., 1990). The labeling of these residues establishes that [^{3}H]chlorpromazine's binding site is within the lumen of the ion channel toward the cytoplasmic end of the pore and helps to identify the pore-lining faces of

This work was supported in part by United States Public Health Service Grant NS19522 and by an award in structural neurobiology from the Keck Foundation.

[1] Present address: Department of Neurology, Washington University School of Medicine, St. Louis, MO 63110.

ABBREVIATIONS: nAChR, nicotinic acetylcholine receptor; HTX, *dl*-perhydrohistrionicotoxin; PAGE, polyacrylamide gel electrophoresis; NCA, noncompetitive antagonist; EKC, endoproteinase Lys-C; 1-AP, 1-azidopyrene; V8 protease, *Staphylococcus aureus* glutamyl endopeptidase; TFA, trifluoroacetic acid; OPA, *o*-phthalaldehyde; PTH, phenylthiohydantoin; [^{125}I]TID, 3-(trifluoromethyl)-3-(*M*-[^{125}I]iodophenyl)diazirine; TPS, *Torpedo* physiological saline.

the M2 segments. In contrast, in the desensitized nAChR, the NCA [^{3}H]meproadifen mustard reacts specifically with αGlu^{262} at position 20 at the extracellular end of the pore (Pedersen et al., 1992).

Unlike chlorpromazine and meproadifen, the uncharged NCA 3-(trifluoromethyl)-3-(*M*-[^{125}I]iodophenyl)diazirine ([^{125}I]TID) binds with similar affinity to both the resting and desensitized states (White et al., 1991) and therefore is a useful probe of the channel in the absence as well as the presence of agonist. In the absence of agonist, [^{125}I]TID specifically photoincorporates into M2 residues at positions 9 and 13, whereas in the desensitized state, it labels residues deeper in the pore (positions 2 and 6) as well as the residues at 9 and 13 (White and Cohen, 1992). This study directly demonstrated a structural change in the pore between resting (closed channel) and desensitized states and suggested that the aliphatic residues at position 9 from each subunit associate in the lumen to provide the permeability barrier in the closed channel.

To better characterize the structure of the ion channel in the closed state, we identified the binding site of the NCA [^{3}H]tetracaine, in the absence of agonist. Unlike the NCAs used in previous photoaffinity labeling studies, tetracaine binds to the nAChR with high affinity in the absence of agonist (K_{eq} = 0.3 μM) and with 100-fold lower affinity in the presence of agonist (Blanchard et al., 1979). Middleton et al. (1999) established that [^{3}H]tetracaine binds with a 1:1 stochiometry to the nAChR and that ultraviolet irradiation at 302 nm resulted in specific [^{3}H]tetracaine photoincorporation into each subunit. We report here the identification of the individual amino acids of the nAChR that photoincorporated [^{3}H]tetracaine. These data show that the high-affinity [^{3}H]tetracaine-binding site is located within the lumen of the ion channel. The labeled amino acids define the surface of the M2 helix extending one helical turn above and below position 9 from each subunit that lines the lumen of the channel in the absence of agonist.

Experimental Procedures

Materials. [^{3}H]Tetracaine was prepared at New England Nuclear Research Products (Boston, MA) by palladium/charcoal-catalyzed reduction in 3,5-dibromotetracaine with carrier-free $^3H_2$ gas. [^{3}H]Tetracaine was purified from the tritium reduction products by silica thin-layer chromatography (5:4:1 cyclohexane/chloroform/diethylamine; R_f = 0.17). The purity (>90%) and specific activity (48 Ci/mmol) were determined by silica HPLC (Hibar Si-60 10 μm, 200:1 acetonitrile/diethylamine isocratic elution). nAChR-rich membranes were isolated from electric organs of *Torpedo californica* (Marinus Inc., Westchester, CA) as described previously (Pedersen et al., 1992) and stored at −80°C in 38% sucrose. Endoproteinase Lys-C (EKC) was obtained from Boehringer-Mannheim (Indianapolis, IN). *l*-1-Tosylamido-2-phenylethylchloromethylketone-treated trypsin was obtained from Worthington Biochemical (Freehold, NJ). *Staphylococcus aureus* glutamyl endopeptidase (V8 protease) was purchased from ICN Biomedical Inc. (Costa Mesa, CA). Oxidized glutathione and tricine were from Sigma Chemical Co. (St. Louis, MO). *o*-Phthalaldehyde (OPA), 10% Genapol C-100, and trifluoroacetic acid (TFA) were obtained from Pierce Chemical Co. (Rockford, IL). 1-Azidopyrene (1-AP) was purchased from Molecular Probes (Eugene, OR). *dl*-perhydrohistrionicotoxin (HTX) was kindly provided by Dr. Y. Kishi (Harvard University, Cambridge, MA).

Photolabeling of nAChR-Rich Membranes with [^{3}H]Tetracaine and Isolation of Labeled nAChR Subunits. Freshly thawed suspensions of nAChR-rich membranes (10–14 mg protein) were diluted 1:2 in *Torpedo* physiological saline (TPS; 250 mM NaCl, 5 mM KCl, 3 mM $CaCl_2$, 2 mM $MgCl_2$, 5 mM NaPi, pH 7.0) and pelleted (15,000*g*) for 30 min at 4°C. The membrane pellets were then resuspended at ~2 mg protein/ml in TPS supplemented with 50 mM oxidized glutathione (Middleton et al., 1999). [^{3}H]Tetracaine was then added at a final concentration of 5 μM, as well as 30 μM HTX for the samples used to define nonspecific photolabeling. The suspensions (2.5-ml volumes) were incubated for 30 min at room temperature with stirring in covered glass crystallization dishes (3 cm diameter) that were flushed with Ar(g) for 15 min immediately before photolysis. The samples, contained in a water bath that served to keep the sample temperature below 25°C, were then irradiated at 302 nm for 30 min with stirring. The lamp (Spectroline model EB-280C; Spectronics, Westbury, NY) was at a distance of 12 cm and had an intensity of ~1000 μW/cm^2 (as measured by a Spectroline DIX 300 digital radiometer). After irradiation, samples were pelleted, resuspended to ~2 mg/ml in TPS, and photolabeled as described (Blanton and Cohen, 1994) with the fluorescent, hydrophobic probe 1-AP. The membranes were then pelleted and resuspended in electrophoresis sample loading buffer for isolation of nAChR subunits by SDS-polyacrylamide gel electrophoresis (PAGE). Labeling with 1-AP was used to facilitate the initial identification and isolation of nAChR subunits and for the subsequent isolation of their hydrophobic fragments (Blanton and Cohen, 1994).

SDS-PAGE. nAChR subunits were resolved by SDS-PAGE using the Laemmli buffer system (Laemmli, 1970) with 1.5-mm-thick, 8% acrylamide slab gels containing 0.32% bisacrylamide. After electrophoresis, the unstained gels were illuminated on a 365-nm UV light box, and the nAChR subunits were visualized by 1-AP fluorescence. The nAChR β, γ, and δ subunits were excised from the gel and eluted in 10 ml of elution buffer (0.1 M NH_4HCO_3/0.1% SDS). The band containing the nAChR α subunit was excised from the gel and placed on top of the stacking portion of a 15% mapping gel for in gel digestion with *S. aureus* V8 protease (Pedersen et al., 1986). The α subunit V8 protease fragments of 20 kDa (αV8–20, αSer^{173}-αGlu^{338}) and 10 kDa (αV8–10; αAsn^{339}-αGly^{437}) were visualized by 1-AP fluorescence (Blanton and Cohen, 1994), excised from the gel, and eluted as above. After 4 days of elution, subunits (or subunit fragments) were concentrated with Centriprep-30 (or -10) Microconcentrators (Amicon, Beverly, MA) to approximately 400 μl, and excess SDS was removed by acetone precipitation at −20°C. The precipitates were resuspended in 15 mM Tris (pH 8.1)/0.1% SDS at 0.4 mg protein/ml. Protein concentration was measured using a bicinchoninic acid-based protein assay (Micro BCA Protein Assay, Pierce Chemical Co.), and [^{3}H]tetracaine incorporation was determined by scintillation counting.

Purification of Proteolytic Digests of [^{3}H]Tetracaine/1-AP-Labeled nAChR Subunits. nAChR αV8–20 and δ subunit at 0.4 to 0.6 mg protein/ml in 15 mM Tris (pH 8.1)/0.1% SDS were digested with 4 U/ml EKC or with 1:1 (w/w) *S. aureus* V8 protease at ambient temperature. The β and γ subunits were digested with trypsin (25% w/w) at ambient temperature in 15 mM Tris (pH 8.1)/0.1% SDS supplemented with 0.5% Genapol C-100. The digestion times are indicated in the figure legends. The proteolytic digests were fractionated by Tricine SDS-PAGE as described (Schagger and von Jagow, 1987; Blanton and Cohen, 1994). To identify regions of the gel that contained specifically labeled fragments, an aliquot (5 μg) of each digest was run in a separate lane of the 1.5-mm-thick preparative gel, and another lane contained prestained molecular weight standards (Life Technologies, Gaithersburg, MD): insulin B (2300) and A (3400) chains, bovine trypsin inhibitor (6200), lysozyme (14,300), α-lactoglobulin (18,400), carbonic anhydrase (29,000), and ovalbumin (43,000). The analytical lanes were cut into 3-mm slices and placed into scintillation tubes. After dissolution of the acrylamide in 800 μl of 30% H_2O_2 heated to 80°C for more than 1 h, the ^{3}H in each sample was determined by scintillation counting in Dimiscint (National Diagnostics, Atlanta, GA).

Bands of the preparative gel were excised based on the observed distribution of ^{3}H in the analytical lanes in relation to molecular weight markers, as well as the visualization of 1-AP fluorescence. The excised bands were diced and passively eluted into 4 ml of elution buffer, and each eluate was concentrated using Centricon-3 Microconcentrators (Amicon).

[^{3}H]Tetracaine/1-AP-labeled fragments were further purified by reversed phase HPLC on a Brownlee C4 Aquapore column (100 × 2.1 mm, 7-μm particle size) as described previously (Pedersen et al., 1992). Solvent A consisted of 0.08% TFA in water, and solvent B consisted of 60% acetonitrile/40% 2-propanol/0.05% TFA. The fragments were eluted at 0.2 ml/min with a linear gradient from 25 to 100% B in 80 min. The elution of peptides was monitored by the absorbance at 210 nm and by fluorescence emission at 432 nm (355-nm excitation), corresponding to the excitation and emission maxima of 1-AP. Fractions (0.5 ml) were collected in plastic tubes, and the distribution of ^{3}H was determined by scintillation counting of 5% of each fraction.

Sequence Analysis. N-terminal sequence analysis was performed on an ABI model 477A (Applied Biosystems, Foster City, CA) protein sequencer with gas phase cycles. HPLC fractions that contained specifically labeled material were pooled and dried by vacuum centrifugation. The dried samples were resuspended in 25 μl of 100 mM NH_4HCO_3/0.05% SDS and then loaded onto chemically modified glass-fiber disks (Beckman, Palo Alto, CA) that were used rather than polybrene-treated filters to improve the sequencing yields of hydrophobic peptides (Pedersen et al., 1992). Before beginning the Edman degradation cycles, the sample in the sequencer cartridge was exposed to TFA vapor for 4 min to fix the sample to the filter, and then SDS was removed by a 5-min wash of the filter with ethyl acetate. Approximately 30% of each degradation cycle was injected into the on-line ABI model 120 A amino acid analyzer to determine the identity of the released phenylthiohydantoin (PTH)-amino acid derivatives, and 60% was delivered to a fraction collector for scintillation counting. During the sequencing of samples containing β-M1, sequencing of contaminating peptides was blocked by treatment of the sample on the filter with OPA. OPA reacts with primary, but not secondary amines, and can be used to block Edman degradation of any peptide not containing an N-terminal proline (Brauer et al., 1984). OPA treatment was carried out as described previously (Middleton and Cohen, 1991). The Applied Biosystem model 610A Data Analysis Program Version 1.2.1 was used to analyze the sequencer chromatograms and calculate the background-subtracted amount of PTH-amino acid present in each cycle of Edman degradation. Initial peptide mass (I_0) and repetitive yield (R) were determined by nonlinear least-squares regression (Sigma Plot) of the function $I = I_0 \times R^n$, where I is the observed mass of PTH-derivative at cycle n. The background-subtracted mass of the PTH derivatives of Ser, Cys, Arg, His, and Trp were excluded from the fits because of known problems of measuring their mass yields.

Results

To identify the amino acids of the nAChR that specifically photoincorporated [^{3}H]tetracaine, we labeled nAChR-rich membranes (5 mg protein, 2 mg/ml) equilibrated with 5 μM [^{3}H]tetracaine in both the absence and presence of 30 μM HTX. The nAChR subunits were purified in good yield (typically 100–200 μg). Then β, γ, and δ subunit preparations each incorporated about 1800 to 2000 ^{3}H cpm/μg protein, with β subunit labeling ~75% specific (i.e., inhibitable by HTX) and γ and δ subunit labeling ~55 and ~70% specific. Although intact α subunit was not routinely isolated, preparations of αV8–20 incorporated ~2500 ^{3}H cpm/μg with an 80% reduction for αV8–20 isolated from nAChRs labeled with [^{3}H]tetracaine in the presence of HTX. The levels of HTX-inhibitable ^{3}H incorporation in each subunit indicated specific incorporation of [^{3}H]tetracaine in ~0.1% of subunits, a level somewhat lower than that seen in the analytical experiments of Middleton et al. (1999).

[^{3}H]Tetracaine Photoincorporation in δ Subunit. In initial experiments, we performed a series of analytical scale digests (5-μg aliquots of labeled δ subunit) with EKC that were analyzed both by the ^{3}H distribution after Tricine SDS-PAGE and by the profile of ^{3}H release when the total digest was sequenced. Digestion conditions that resulted in a fragment (or fragments) releasing ^{3}H after 9 and 13 cycles of Edman degradation were identified (not shown). The digest contained a single, specifically labeled fragment of ~10 kDa, as shown in Figure 1A, the analytical lanes (5-μg aliquots) of a preparative scale digest of δ subunits (~150 μg protein) isolated from nAChRs labeled in the absence or presence of HTX. The peak of ^{3}H corresponded to a band of 1-AP fluorescence in the preparative lanes and a 5-mm strip contain-

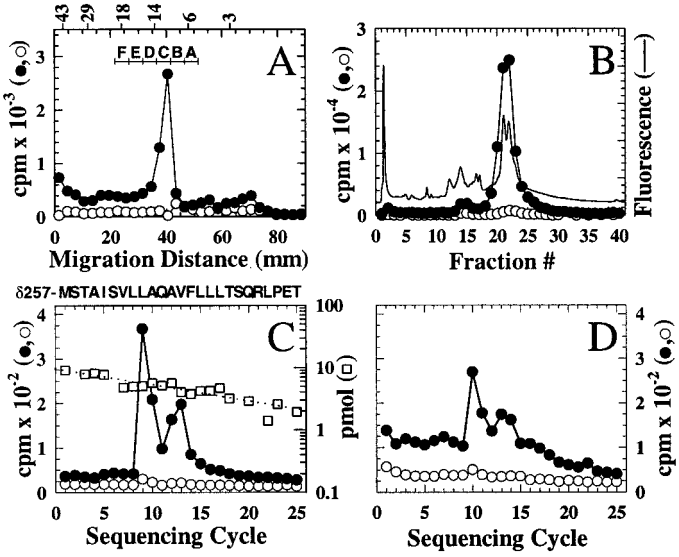

Fig. 1. Proteolytic mapping of [^{3}H]tetracaine incorporation in nAChR δ subunit with endoproteinase Lys-C (A–C) or *S. aureus* V8 protease (D). All panels display results from parallel photolabelings of nAChR-rich membranes with [^{3}H]tetracaine in the absence (●) or presence (○) of HTX. Solutions (0.4 mg/ml) of [^{3}H]tetracaine-labeled δ subunit were digested with EKC (3U/ml) for 5 days at ambient temperature and fractionated by Tricine SDS-PAGE with 5-μg aliquots (−HTX, 10,780 cpm; +HTX, 3050 cpm) electrophoresed in analytical lanes adjacent to the bulk digests. A, distribution of ^{3}H in the analytical lanes is shown in relation to molecular weight markers (above) and the strips (A–F) excised from the preparative lanes. For the −HTX sample, 543,300 cpm was loaded onto the preparative lane, with 14,640, 17,000, 66,560, 31,640, 11,520, and 7600 cpm recovered from strips A to F, respectively. The eluates from strips C and D were combined and designated as δEKC-10. B, reversed phase HPLC purification of δEKC-10 (5% of the HPLC fractions) were assayed for ^{3}H. Specifically labeled material (66% of loaded cpm) eluted in a single peak (fractions 20–23). Fractions 21 and 22 were pooled for sequence analysis. C, ^{3}H and mass release on N-terminal sequencing of δEKC-10 purified by reversed phase HPLC. The only sequence detected in either sample began at δMet^{257}, the N terminus of δM2 (□, −HTX, I_0 = 10 pmol, R = 94%, 10,000 cpm loaded/1800 cpm remained on the filter; +HTX, I_0 = 11 pmol, R = 94%). The sequence of the identified peptide is shown above. D, ^{3}H release from N-terminal sequencing of δV8–3. Solutions of [^{3}H]tetracaine-labeled δ subunit (0.6 mg/ml) were digested with an equal weight of *S. aureus* V8 protease for 14 days at ambient temperature and then separated by Tricine SDS-PAGE (not shown). A 3-kDa specifically labeled fragment (δV8–3) was excised, purified by reversed phase HPLC (not shown), and sequenced (−HTX, 13,700 cpm loaded/2300 cpm remained on the filter). As many as five different PTH derivatives were identified in each cycle of Edman degradation.

ing the fluorescent band, as well as sections below and above the fluorescent band, were excised from each preparative lane, and the protein in them was eluted. The eluates from the fluorescent band (band C) and the band above (band D) contained the highest amounts of ^{3}H, which when combined accounted for 38% of the eluted cpm. The material eluted from these two sections was pooled and is referred to as δEKC-10.

When δEKC-10 was further purified by reversed phase HPLC (Fig. 1B), about 66% of ^{3}H loaded on the column eluted in a single peak of ^{3}H centered at 65% organic that was associated with two peaks of fluorescence. For δEKC-10 from nAChRs labeled with [^{3}H]tetracaine in the presence of HTX, the ^{3}H in that peak was reduced by >95% (Fig. 1B), whereas the peaks of fluorescence were similar in magnitude (not shown). Sequence analysis (Fig. 1C) of the pooled fractions (f21–22) from both the specifically and nonspecifically labeled δEKC-10 fragments revealed the presence of a single peptide starting at δ-Met^{257} at the N terminus of M2 (−HTX, I_0 = 10 pmol; +HTX, 11 pmol). No other sequences were identifiable, with other PTH amino acids present at less than 5% the level of the primary sequence. The molecular weight of this fragment and its labeling by 1-AP (Blanton and Cohen, 1994) indicated that it must extend through the M3 hydrophobic segment. The ^{3}H release profile revealed clear peaks of ^{3}H release in cycles 9, 12, and 13 that were reduced by more than 90% for the sample labeled in the presence of HTX. The release of ^{3}H in those cycles correspond to [^{3}H]tetracaine reaction with δLeu^{265}, δAla^{268}, and δVal^{269}.

Although only one fragment beginning at the N terminus of δM2 was identified in the sequence analysis of δEKC-10, it was possible that the observed ^{3}H release originated from a contaminating peptide present at levels below detection (<0.5 pmol). Therefore, we used a second digestion strategy to verify that the ^{3}H release in cycles 9, 12, and 13 originated from δLeu^{265}, δAla^{268}, and δVal^{269} and not from a contaminating peptide. Digestion with V8 protease could result in cleavage at δGlu^{255} and at δGlu^{280} at the N and C termini of δM2, which would generate a ~2.9-kDa fragment. Following cleavage after δGlu^{255}, ^{3}H release would be expected in cycles 10, 13, and 14 of Edman degradation.

Aliquots (75 μg) of labeled δ subunits were digested with an equal weight of V8 protease for 14 days at room temperature. The digestion products were then purified by Tricine SDS-PAGE, with 5-μg aliquots from each sample loaded in analytical lanes. The ^{3}H distribution in the analytical lanes showed a specifically labeled band at 3 kDa (not shown). This band, referred to as δV8–3, was eluted and purified by reversed phase HPLC (not shown). Sequence analysis revealed the presence of at least five different peptides in δV8–3. However, in the ^{3}H release profile, there was specific release of ^{3}H in cycles 10, 13, and 14 (Fig. 1D), a result consistent with labeling at δLeu^{265}, δAla^{268}, and δVal^{269} after V8 protease cleavage at δGlu^{255}. The observed molecular weight of this labeled peptide as well as the ^{3}H release pattern were as predicted for specific [^{3}H]tetracaine incorporation within δM2.

[^{3}H]Tetracaine Photoincorporation in β Subunit. White and Cohen (1992) showed that digestion of [^{125}I]TID-labeled β subunit with trypsin generated a 7-kDa fragment beginning at the N terminus of βM2 and extending through the M3 segment, as well as 3- and 10-kDa fragments that also contained βM2. Therefore, we digested [^{3}H]tetracaine-labeled β subunit (160 μg, 290,000 cpm) with trypsin [25% (w/w)] for 4 days at ambient temperature and then purified the digestion products by Tricine SDS-PAGE. Aliquots (5 μg) were electrophoresed in analytical lanes adjacent to the bulk digest. The ^{3}H distribution in these analytical lanes (Fig. 2A) showed that specifically labeled material migrated in bands at 7 and 3 kDa. Material was eluted from gel strips (bands A–G) that were excised from the preparative lanes that spanned from below the 3-kDa marker to above the 14-kDa marker. Bands B and C, which contained 54,000 cpm (19% of loaded counts), were combined and denoted βT-3, and bands E and F, which contained 52,000 cpm (18% of loaded counts), were combined and denoted βT-7.

The material eluted from βT-7 was further purified by HPLC (Fig. 2B). The specifically labeled material was recovered in a single peak (fractions 22–24) that was associated with two peaks in absorbance. For the nonspecifically labeled sample, the ^{3}H in those fractions was <10% that of the specifically labeled sample, whereas the absorbance peaks were similar to those for the specifically labeled sample.

Sequence analysis of HPLC purified βT-7 (Fig. 2C) revealed the presence of a primary sequence beginning at βMet^{249} at the N terminus of βM2 (I_0 = 13 pmol) and a secondary sequence beginning at βLys^{216} at the N terminus of βM1 (I_0 = 6 pmol). There was a clear peak of release of ^{3}H in cycle 9 that was reduced by >95% for the sample labeled nonspecifically. If the release in cycle 9 originated from the primary sequence (βM2), it would indicate labeling of βLeu^{257}, the amino acid homologous to the major site of labeling in δ subunit (δLeu^{265}).

To test whether the ^{3}H release in cycle 9 during the sequencing of βT-7 was from the βM2 or the βM1 domain, the βT-3 band was also analyzed. When the βT-3 band was purified by HPLC (Fig. 2D), material was recovered in three overlapping peaks of ^{3}H. The largest peak (denoted βT-3a), which accounted for 35% of the loaded cpm, was centered at 52% organic, and a second peak (denoted βT-3b), which accounted for 22% of the loaded ^{3}H, eluted at ~59% organic. βT-3a eluted in the HPLC gradient where White and Cohen (1992) previously recovered a 3-kDa fragment of the βM2 domain, whereas βT-3b eluted close to the reported position of βM1 (Blanton and Cohen, 1994).

Sequence analysis of βT-3a revealed ^{3}H release only in cycle 9, as was seen for βT-7. However, the presence of at least four different sequences, including autodigestion products of trypsin, precluded direct fragment identification (not shown). For βT-3b, a sequencing protocol was used to determine whether any ^{3}H release originated from the βM1 segment. To selectively sequence βM1 in a sample likely to contain other β subunit fragments, OPA, a compound that selectively blocks primary but not secondary amines (proline), was applied before the second sequencing cycle where βPro^{217} was expected to be exposed. This treatment will block the Edman degradation of all peptides that do not contain an N-terminal proline residue. After OPA treatment at cycle 2, the only observed sequence began at βPro^{217} (βM1) which was present at an initial mass of 1 pmol (Fig. 2E), and there was no ^{3}H release above background. At this mass of βM1, one would have expected to see 70 cpm of ^{3}H release at cycle 9 if the ^{3}H release seen in the sequencing of βT-7 (Fig. 2C) corresponded to βThr^{224} (in β-M1) and not βLeu^{257} (in

βM2). Because the sequencing of βT-3b demonstrated that there was no ^{3}H release at cycle 9 in βM1, we conclude that βLeu^{257} (in βM2) is labeled and not βThr^{224}.

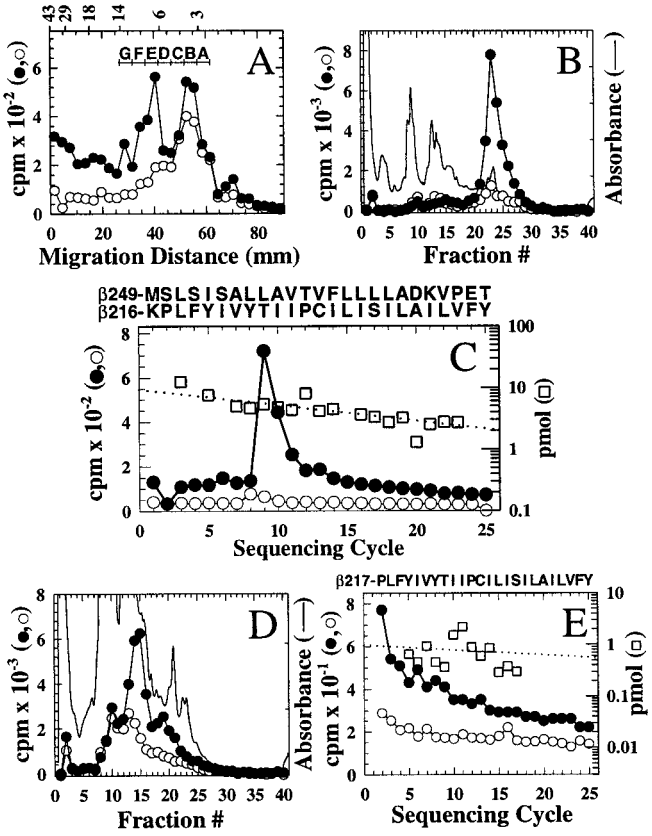

Fig. 2. Proteolytic mapping with trypsin of [^{3}H]tetracaine incorporation in the nAChR β subunit. All panels display results from parallel photolabelings of nAChR-rich membranes with [^{3}H]tetracaine in the absence (●) or presence (○) of HTX. Solutions (0.7 mg/ml) of [^{3}H]tetracaine-labeled β subunit were digested with trypsin (0.2 mg/ml) for 4 days at ambient temperature and then fractionated by Tricine SDS-PAGE with 5-μg aliquots (−HTX, 9000 cpm; +HTX, 2630 cpm) electrophoresed in analytical lanes adjacent to the bulk digests. A, distribution of ^{3}H in the analytical lanes is shown in relation to molecular weight markers (above) and the strips (A–G) excised from the preparative lanes. For the −HTX sample, 213,600 cpm was loaded on the preparative lane, with 19,200, 29,200, 25,000, 20,450, 25,650, 26,350, and 12,850 cpm recovered from strips A to G, respectively. The eluates from strips B and C (~3 kDa) were combined and designated as fragment βT-3, and the eluates from strips E and F (~7 kDa) were combined and designated as fragment βT-7. B and D, reversed phase HPLC purification of βT-7 and βT-3 (5% of the HPLC fractions were assayed for ^{3}H). B, for βT-7 (−HTX), 46% of the 51,000 cpm injected was recovered in a single peak associated with two absorbance peaks. Fractions 22 to 24 were combined for sequence analysis. D, for βT-3 (−HTX), specifically labeled material eluted in three peaks that together accounted for 70% of the injected ^{3}H. Fractions 13 to 15 (βT-3a, 30% of injected ^{3}H) and fractions 16 to 19 (βT-3b, 20% of injected ^{3}H) were pooled for sequence analysis. C, ^{3}H and mass release on N-terminal sequencing of βT-7 purified by reversed phase HPLC. For both samples, the primary sequence began at βMet^{249}, the N terminus of βM2 (□, −HTX, I_0 = 13 pmol, R = 92%, 16,420 cpm loaded/3180 cpm remained on the filter; +HTX, I_0 = 12 pmol, R = 96%), and a secondary sequence began at βLys^{216}, the N terminus of βM1 (−HTX, I_0 = 6 pmol, R = 92%; +HTX, I_0 = 8 pmol, R = 95%). The sequences of the identified peptides are shown above. Additional PTH derivatives were present at <20% the level the primary sequence. E, sequence analysis of βT-3b. After one cycle of Edman degradation, the sequencing filter was treated with OPA, which reacts selectively with the free N termini of amino acids other than proline, a secondary amine, blocking Edman degradation (Brauer et al., 1984). After OPA block, the primary sequence in both samples began at βLys^{216}, the N terminus of βM1 (−HTX, I_0 ~ 1 pmol, R = 95%, 10,400 cpm loaded/410 cpm remained on the filter). The sequence of the identified peptide is shown above.

[^{3}H]Tetracaine Photoincorporation in α Subunit. The specific [^{3}H]tetracaine photolabeling in the α subunit is contained within αV8–20 (Ser^{162}/Ser^{173} to Glu^{338}/Asn^{339}), a proteolytic fragment produced by an "in gel" digest of α subunit with V8 protease (Middleton et al., 1999). To determine whether that specific labeling was within αM2, [^{3}H]tetracaine-labeled αV8–20 was digested with endoproteinase Lys-C, which had been used previously (Pedersen et al., 1992) to generate an ~8-kDa fragment beginning at the N terminus of αM2 in studies of the site of labeling of [^{3}H]meproadifen mustard. When the EKC digest was fractionated by Tricine SDS-PAGE, the distribution of ^{3}H in the analytical lanes (Fig. 3A) contained a peak of specifically labeled material migrating at ~8 kDa, as well as material aggregated near the top of the gel and a band of ~14 kDa. The preparative lanes of the gels were cut into strips (re-

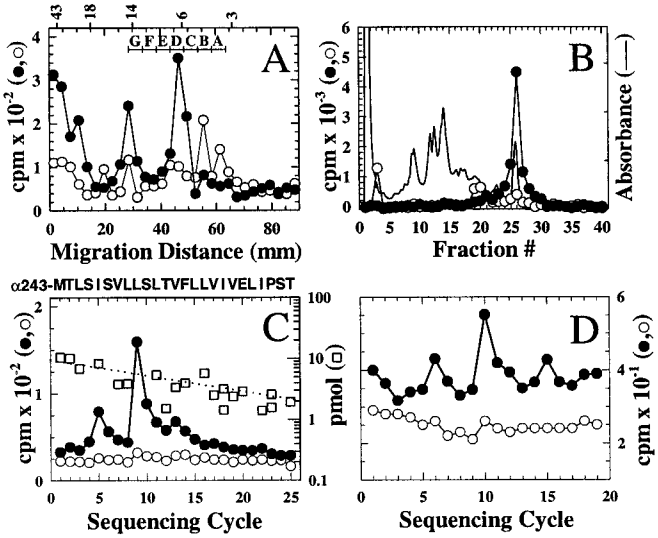

Fig. 3. Proteolytic mapping of [^{3}H]tetracaine incorporation in the nAChR α subunit with endoproteinase Lys-C (A–C) or *S. aureus* V8 protease (D). All panels display results from parallel photolabelings of nAChR-rich membranes with [^{3}H]tetracaine in the absence (●) or presence (○) of HTX. Solutions (0.6 mg/ml) of αV8–20 isolated from [^{3}H]tetracaine-labeled α subunit were digested with EKC (3 U/ml) for 6 days at ambient temperature and fractionated by Tricine SDS-PAGE with 5-μg aliquots (−HTX, 16,060 cpm; +HTX, 3315 cpm) electrophoresed in analytical lanes adjacent to the bulk digests. A, the distribution of ^{3}H in the analytical lanes is shown in relation to molecular weight markers (above) and the strips (A–G) excised from the preparative lanes. For the −HTX sample, 73,900 cpm was loaded on the preparative lane, with 1550, 2750, 2050, 7150, 7550, 2000, and 1850 cpm recovered from strips A to G, respectively. The eluates from strips D and E were combined and designated as αEKC-8. B, reversed phase HPLC purification of αEKC-8 (5% of the HPLC fractions were assayed for ^{3}H). For the −HTX sample, 50% of the 14,000 cpm injected was recovered in a single peak associated with a single peak in absorbance and fluorescence (not shown). Fractions 25 to 27 were combined for sequence analysis. C, ^{3}H and mass released from N-terminal sequencing of αEKC-8 purified by reversed phase HPLC. The only sequence detected in either sample began at αMet^{243}, the N terminus of αM2 (□, −HTX, I_0 = 11 pmol, R = 86%, 6740 cpm loaded/680 cpm remained on the filter; +HTX, I_0 = 27 pmol, R = 86%). The sequence of the identified peptide is shown above. This sequence was present at a 10-fold higher level than any secondary sequence. D, ^{3}H release on N-terminal sequencing of an *S. aureus* V8 protease digest of αV8–20. Solutions of [^{3}H]tetracaine-labeled αV8–20 (0.3 mg/ml) were further digested with equal weight of V8 protease for 28 days at ambient temperature and then separated by reversed phase HPLC (not shown). The ^{3}H peak (43% of recovered ^{3}H), which eluted at 88% organic, was sequenced (−HTX, 14,500 cpm loaded/3640 cpm remained on the filter). The presence of multiple PTH derivatives in each cycle of Edman degradation precluded the identification of peptides in this sample.

ferred to as bands A–G), which together spanned the gel from below the 6-kDa marker to above the 14-kDa molecular weight marker. For the digest of αV8–20 labeled in the absence of HTX, 14,000 cpm of the 74,000 cpm loaded on the gel was recovered from bands D and E. This material, which was combined and denoted as αEKC-8, accounted for 40% of the ^{3}H cpm eluted. When αEKC-8 was further purified by HPLC (Fig. 3B), 50% of the loaded cpm was recovered in a single peak (fractions 25–27) associated with single peaks in fluorescence and absorbance. For the sample labeled in the presence of HTX, the ^{3}H in that peak was reduced by >90%, whereas the peaks in fluorescence and absorbance were similar in size to those seen for the specifically labeled sample (not shown).

Sequence analysis of HPLC-purified αEKC-8 (Fig. 3C) revealed the presence of a peptide beginning at αMet^{243} at the N terminus of αM2 (−HTX, I_0 = 11 pmol; +HTX, I_0 = 27 pmol), with any other sequence present at <10% that level. The major peak of ^{3}H release was in cycle 9 (αLeu^{251}), with lower level ^{3}H release in cycles 5 (αIle247) and 13 (αVal-255). The observed ^{3}H release resulted from specific [^{3}H]tetracaine photolabeling, since the ^{3}H release was reduced by >90% in the sample isolated from nAChR photolabeled in the presence of HTX.

An alternative digestion strategy using *S. aureus* V8 protease in conjunction with radiochemical sequencing also led to the conclusion that αIle^{247} and αLeu^{251} were the amino acids specifically photolabeled by [^{3}H]tetracaine. There is a potential cleavage site for V8 protease at αGlu^{241} immediately preceding αLys^{242} that was the site of cleavage by EKC. [^{3}H]Tetracaine-labeled αV8–20 was digested for 28 days with an equal weight of *S. aureus* V8 protease, and the digest was then fractionated by HPLC. Radioactivity (34% of eluted cpm) was recovered in a peak centered at 88% organic that was sequenced for 25 cycles (Fig. 3D). Although the presence of multiple PTH derivatives in each sequencing cycle prevented identification of the fragments present, there was ^{3}H release in cycles 6, 10, and 15. Release in cycles 6 and 10 was consistent with the ^{3}H release seen in cycles 5 and 9 in the sequencing of αEKC-8. The lack of significant ^{3}H release in cycle 14 was not surprising, based on the relative levels of ^{3}H release in cycles 9 and 13 in the sequencing of αEKC-8. Release in cycle 15 was unexpected. It might result from labeling of αVal255 with release in cycle 15 rather than 14 due to low repetitive yield of Edman degradation, but it could also result from [^{3}H]tetracaine photoincorporation in another, unidentified fragment.

[^{3}H]Tetracaine Photoincorporation in γ Subunit. Attempts to isolate a labeled fragment of γ subunit were unsuccessful. Digestion of intact γ subunit with either endoproteinase Lys-C or trypsin resulted in specifically labeled fragment or fragments of <3 kDa, which when repurified by HPLC eluted in common with many peptides. After digestion of γ subunit (170 μg) with trypsin, 31% of the specifically labeled material migrated in a band below 3 kDa (γT-3), a result consistent with the presence of trypsin sites at the N and C termini of γM2. When further purified by reversed phase HPLC, 34% of the specifically labeled cpm were recovered in a peak centered at 48% organic, consistent with a previously characterized 3-kDa peptide containing M2 (White and Cohen, 1992). Sequence analysis of HPLC-purified γT-3 revealed the presence of a complex mixture of unidentifiable peptides. There was a peak of ^{3}H release in cycle 9 (40 cpm), which, if it originated from γM2, would correspond to γLeu^{260}, the amino acid homologous to the most highly labeled amino acids in the other subunits.

Discussion

In this report, we mapped the binding site for [^{3}H]tetracaine in the closed channel state of the *Torpedo* nAChR by identifying the amino acids specifically photolabeled by this drug. N-terminal sequencing demonstrated that the specific photoincorporation within the α, β, and δ subunits was contained within proteolytic fragments that included the M2 segments. Sites of specific ^{3}H release in these fragments corresponded to labeling within the M2 segments of αIle^{247}, αLeu^{251}, αVal^{255}, βLeu^{257}, δLeu^{265}, δAla^{268}, and δVal^{269}. Trypsin digestion of labeled γ subunit produced a labeled proteolytic fragment whose size and hydrophobicity were consistent with the known properties of isolated M2 segments, and sequence analysis of this material showed release of ^{3}H nine cycles after the N terminus that, if originating from γM2, corresponds to γLeu260.

Each of the labeled residues lies on a common helical face of the M2 segments (Fig. 4A). Because [^{3}H]tetracaine binds to the nAChR with a 1:1 stoichiometry (Middleton et al., 1999), the photolabeling data provide clear evidence that this binding site is located within the lumen of the closed ion channel and identify the amino acids within M2 that are in close proximity to bound tetracaine. Although [^{125}I]TID labels many of the same residues (White and Cohen, 1992), the additional residues labeled by [^{3}H]tetracaine (αIle^{247}, δAla^{268}) extend the definition of the surface of the M2 helix that is oriented toward the lumen of the closed ion channel (Fig. 4B; [^{3}H]tetracaine: δ arc = 100 degrees, α arc = 80 degrees; [^{125}I]TID: α, β, δ arcs = 40 degrees).

The photochemistry of [^{3}H]tetracaine is unknown. However, the photolysis products of *para*-aminobenzoic acid (Chignell et al., 1980; Gasparro, 1985) include reactive radicals at the aromatic nitrogen and on the adjacent carbon on the benzene ring. This suggests that reactive radicals should be produced at tetracaine's aromatic atoms as well. In the model in Figure 4A, tetracaine has been aligned with its benzene ring positioned at the level of M2 position 9 (i.e., at the level of the amino acids that are the most efficiently labeled in each M2 segment). In this orientation, tetracaine's benzene ring, as well as its aryl nitrogen and carboxyl, could interact with the labeled residues at positions 5, 9, 12, and 13 and account for all the specific photolabeling. With the benzene ring at this position, chemical intuition suggests that it would be energetically favorable for tetracaine to be oriented as shown with its *N*-butyl substituent interacting with the hydrophobic residues at positions 16 and 17 (leucines, valines, and phenylalanines) and the dimethylamino group (probably protonated) interacting with hydrophilic side chains (serines and threonines) at position 6.

An orientation of tetracaine with its *N*-butyl group interacting with the hydrophobic residues at positions M2–16 and M2–17 is consistent with structure-activity studies of tetracaine analogs. Procaine, a tetracaine analog that lacks the butyl group on the aryl nitrogen, is bound by the *Torpedo* nAChR in the absence of agonist with 1000-fold lower affinity than tetracaine (Middleton et al., 1999). Although the hydro-

phobic side chains at M2–16 and M2–17 would form an energetically favorable environment for the butyl group of tetracaine, no such stabilization would be expected for the unsubstituted aryl nitrogen of procaine. In addition, if the desensitized state of the nAChR has a more open pore structure at the level of positions 2, 6, and 9, as is required to accommodate drugs such as trimethylphenylphosphonium and chlorpromazine and (Hucho et al., 1986; Revah et al., 1990; White and Cohen, 1992), then the dimethylamino of tetracaine may contribute less to the energetics of binding in the desensitized state than does a diethyl group. This interpretation is consistent with the analysis of tetracaine analogs by Middleton et al. (1999). This proposed orientation of bound tetracaine is also consistent with the observation that tetracaine is 10 times more potent as an antagonist of *Torpedo* than of mouse muscle nAChR (Eterovic et al., 1993). The *Torpedo* and mouse muscle nAChRs have nearly identical M2 segments, with substitutions at three positions in β subunit (βS2G, βS6F, βA10T) and one in γ subunit (γS6N). The differences include an increase in hydrophobicity at position 6 in the mouse β subunit. If our model of tetracaine's interaction with the *Torpedo* receptor is correct, then the mouse muscle nAChR may interact less strongly with the charged dimethylamino group of tetracaine.

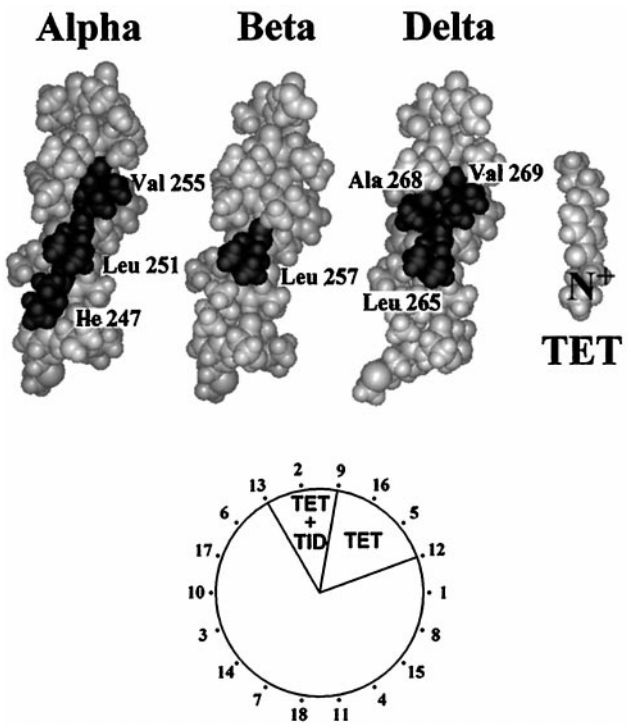

Fig. 4. The pattern of [^{3}H]tetracaine photoincorporation defines the surface of the M2 segments lining the closed channel and suggests a model for tetracaine binding within the nAChR ion channel. A, space-filling, α-helical models of each subunit's M2 segment and a model at the same scale of tetracaine in an extended conformation were made using the molecular modeling software Insight (Biosym, Inc.). The M2 residues labeled by [^{3}H]tetracaine, which are shaded, lie on a single helical face. The presumed photoreactive aromatic atoms of tetracaine are positioned at the same level as the labeled residues of the M2 helices. In this orientation, tetracaine's dimethylaminoethyl group would be in proximity to the hydrophilic side chains at position M2–6, whereas its N-butyl group is aligned with the hydrophobic residues toward the C terminus of the M2-segment. B, when depicted on a helical wheel, the α carbons of the labeled residues in the α subunit (positions 5, 9, and 13) span 80 degrees of the helix cylinder, and those of the δ subunit (positions 9, 12, and 13) span 100 degrees of the helical face. Thus, identification of amino acids labeled by [^{3}H]tetracaine extends the definition of the surface of the M2 helices lining the lumen of the closed channel beyond those side labeled by [^{125}I]TID (residues 9 and 13; White and Cohen, 1992).

The positioning of tetracaine's dimethylamino group near position M2–6 is in apparent contrast to the proposed permeability barrier. Previous mutagenesis (Revah et al., 1991; Filatov and White, 1995; Labarca et al., 1995), electron microscopy (Unwin, 1993, 1995), and photolabeling (White and Cohen, 1992; Blanton et al., 1998) studies have suggested that the hydrophobic side chains at M2–9 could form the permeability barrier in the closed channel. However, the kinetics of [^{3}H]tetracaine binding to the *Torpedo* nAChR in the absence of agonist are characterized by very low association ($k_+ = 4 \times 10^4$ M^{-1} min^{-1}) and dissociation ($k_- = 3 \times 10^{-4}$ s^{-1}) rate constants at 4°C (Cohen et al., 1986; Strnad, 1988). This indicates that tetracaine's access to its high-affinity binding site in the closed channel, as well as its kinetics of dissociation, is greatly hindered and depend on slow changes in the structure of the pore region that are distinct from the movements required for channel opening. In support of this interpretation, TID, which has a much greater association rate constant at 4°C ($k_+ \sim 2 \times 10^6$ M^{-1} min^{-1}; Wu et al., 1994), is not in contact with (i.e., does not label) residues below M2–9 in the absence of agonist.

An alternative model for the permeability barrier, based on the access from the extracellular side of water-soluble sulfhydryl reagents in the absence of agonist to positions as low as M2–2, places the permeability barrier below M2–2 (Akabas et al., 1994; Pascual and Karlin, 1998). However, for 2-aminoethyl methanethiosulfonate, the rate of reaction with a cysteine at position 2 in αM2 was 3×10^4 M^{-1} min^{-1} (Pascual and Karlin, 1998), which is close to the observed association rate constant for [^{3}H]tetracaine binding to *Torpedo* nAChR, whereas the rates of reaction at positions 6, 9, and 10 were 1 to 3×10^3 M^{-1} min^{-1}. Although it is clear that factors other than the kinetics of access do contribute to the rate constant for cysteine alkylation, the observed accessibility and reactivity of cysteines within the M2 channel domain in the absence of agonist are not incompatible with a structural barrier made up by the aliphatic residues at M2–9 that contributes to the hindered binding of tetracaine and to the permeability barrier to inorganic cations in the closed channel. There is no reason to expect that the kinetics of tetracaine association and dissociation from the closed channel would be determined by a structural constraint below the level of position 2 in the M2 domain.

Tetracaine is an unusual NCA in that it binds with 100-fold higher affinity to the resting state than to the desensitized state, and this preferential binding in the absence of agonist emphasizes the restricted dimensions of drugs that can be accommodated within the structure of the closed channel. In the absence of agonist, a benzene ring (~6.5 Å) as well as the butylamino group (~4 Å wide in extended configuration) can be accommodated within the ion channel in a hydrophobic environment that does not exist in the desensitized state of the nAChR. The hindered binding kinetics indicates that the structure of the pore must relax somewhat to accommodate tetracaine, but the change in structure is far smaller than that required for transitions to either the open channel or desensitized state. Although the width of tetracaine may be larger than the restriction in the closed channel in the absence of drug, it is not nearly as large as the desensitizing

NCAs such as chlorpromazine that bind at the level of M2–2 and M2–6 in the desensitized state (Revah et al., 1990). The hydrophobic ring made up by the leucines at M2–9 must be more splayed apart in the desensitized than in the resting state (White and Cohen, 1992), and there is no longer a domain within the pore with a structure favorable for the high-affinity binding of a molecule with tetracaine's dimensions.

Acknowledgments

We thank Dr. David Chiara for his valuable guidance in protein sequencing strategies and for assistance with the preparation of the final figures.

References

Akabas MH, Kaufmann C, Archdeacon P and Karlin A (1994) Identification of acetylcholine receptor channel-lining residues in the entire M2 segment of the alpha subunit. *Neuron* **13:**919–927.

Blanchard SG, Elliott J and Raftery MA (1979) Interaction of local anesthetics with *Torpedo californica* membrane-bound acetylcholine receptor. *Biochemistry* **18:** 5880–5884.

Blanton MP, Dangott LJ, Raja SK, Lala AK and Cohen JB (1998) Probing the structure of the nicotinic acetylcholine receptor ion channel with the uncharged photoactivable compound [^{3}H]diazofluorene. *J Biol Chem* **273:**8659–8668.

Blanton MP and Cohen JB (1994) Identifying the lipid-protein interface of the *Torpedo* nicotinic acetylcholine receptor: Secondary structure implications. *Biochemistry* **33:**2859–2872.

Brauer AW, Oman CL and Margolies MN (1984) Use of *o*-phthalaldehyde to reduce background during automated Edman degradation. *Anal Biochem* **137:**134–142.

Charnet P, Labarca C, Leonard RJ, Vogelaar NJ, Czyzyk L, Gavin A, Davidsen N and Lester HA (1990) An open-channel blocker interacts with adjacent turns of α-helices in the nicotinic acetylcholine receptor. *Neuron* **2:**87–95.

Chignell CF, Kalayanaraman B, Mason RP and Sik RH (1980) Spectroscopic studies of cutaneous photosensitizing agents. I: Spin trapping of photolysis products from sulfanilamide, 4-aminobenzoic acid and related compounds. *Photochem Photobiol* **32:**563–571.

Cohen JB, Correll LA, Dreyer EB, Kuisk IR, Medynski DC and Strnad NP (1986) Interactions of local anesthetics with *Torpedo* nicotinic acetylcholine receptors, in *Molecular and Cellular Mechanisms of Anesthetics* (Roth SH and Miller KW eds) pp 111–124, Plenum Press, New York.

Eterovic VA, Li L, Ferchmin PA, Lee YH, Hann RM, Rodriguez AD and McNamee MG (1993) The ion channel of muscle and electric organ acetylcholine receptors: Differing affinities for noncompetitive inhibitors. *Cell Mol Neurobiol* **13:**111–121.

Filatov GN and White MM (1995) The role of conserved leucines in the M2 domain of the acetylcholine receptor in channel gating. *Mol Pharmacol* **48:**379–384.

Gasparro FP (1985) UV-induced photoproducts of para-aminobenzoic acid. *Photodermatology* **2:**151–157.

Giraudat J, Dennis M, Heidmann T, Chang J-Y and Changeux J-P (1986) Structure of the high-affinity binding site for noncompetitive blockers of the acetylcholine receptor: Serine-262 of the δ subunit is labeled by [^{3}H]chlorpromazine. *Proc Natl Acad Sci USA* **83:**2719–2723.

Giraudat J, Dennis M, Heidmann T, Haumont P-Y, Lederer F and Changeux J-P (1987) Structure of the high-affinity binding site for noncompetitive blockers of the acetylcholine receptor: [^{3}H]Chlorpromazine labels homologous residues in the β and γ chains. *Biochemistry* **26:**2410–2418.

Giraudat J, Gali J-Z, Revah F, Changeux J-P, Haumont P-Y and Lederer F (1989) The noncompetitive blocker [^{3}H]chlorpromazine labels segment M2 but not segment M1 of the nicotinic acetylcholine receptor α subunit. *FEBS Lett* **253:**190–198.

Hucho F, Oberthur W and Lottspeich F (1986) The ion channel of the nicotinic acetylcholine receptor is formed by the homologous helices M II of the receptor subunits. *FEBS Lett* **205:**137–142.

Hucho F, Tsetlin VI and Machold J (1996) The emerging three-dimensional structure of a receptor: The nicotinic acetylcholine receptor. *Eur J Biochem* **239:**539–557.

Imoto K, Busch C, Sakmann B, Mishina M, Konno T, Nakai J, Bujo H, Mori Y, Fukuda K and Numa S (1988) Rings of negatively charged amino acids determine the acetylcholine receptor channel conductance. *Nature (Lond)* **335:**645–648.

Imoto K, Konno T, Nakai J, Wang F, Mishina M and Numa S (1991) A ring of uncharged polar amino acids as a component of channel constriction in the nicotinic acetylcholine receptor. *FEBS Lett* **289:**193–200.

Karlin A and Akabas MH (1995) Toward a structural basis for the function of nicotinic acetylcholine receptors and their cousins. *Neuron* **15:**1231–1244.

Labarca C, Nowak MW, Zhang HY, Tang LX, Deshpande P and Lester HA (1995) Channel gating governed symmetrically by conserved leucine residues in the M2 domain of nicotinic receptors. *Nature (Lond)* **376:**514–516.

Laemmli UK (1970) Cleavage of structural proteins during the assembly of the head of bacteriophage T4. *Nature (Lond)* **227:**680–685.

Middleton RE and Cohen JB (1991) Mapping of the acetylcholine binding site of the nicotinic acetylcholine receptor: [^{3}H]-Nicotine as an agonist photoaffinity label. *Biochemistry* **30:**6987–6997.

Middleton RE, Strnad NP and Cohen JB (1999) Photoaffinity labeling the *Torpedo* nicotinic acetycholine receptor with [^{3}H]tetracaine, a nondesensitizing noncompetitive antagonist. *Mol Pharmacol* **56:**290–299.

Pascual JM and Karlin A (1998) State-dependent accessibility and electrostatic potential in the channel of the acetylcholine receptor: Inferences from rates of reaction of thiosulfonates with substituted cysteines in the M2 segment of the alpha subunit. *J Gen Physiol* **111:**717–739.

Pedersen SE, Dreyer EB and Cohen JB (1986) Location of ligand binding sites on the nicotinic acetylcholine receptor α subunit. *J Biol Chem* **261:**13735–13743.

Pedersen SE, Sharp SD, Liu W-S and Cohen JB (1992) Structure of the noncompetitive antagonist binding site in the *Torpedo* nicotinic acetylcholine receptor: [^{3}H]Meproadifen mustard reacts selectively with α subunit Glu262. *J Biol Chem* **267:**10489–10499.

Revah F, Bertrand D, Galzi JL, Devillers-Thiery A, Mulle C, Hussy N, Bertrand S, Ballivet M and Changeux JP (1991) Mutations in the channel domain alter desensitization of a neuronal nicotinic receptor. *Nature (Lond)* **353:**846–849.

Revah F, Galzi JL, Giraudat J, Haumont P-Y, Lederer F and Changeux J-P (1990) The noncompetitive blocker [^{3}H]chlorpromazine labels three amino acids of the acetylcholine receptor γ subunit: Implications for the α-helical organization of regions MII and for the structure of the ion channel. *Proc Natl Acad Sci USA* **87:**4675–4679.

Schagger H and von Jagow G (1987) Tricine-sodium dodecyl sulfate-polyacrylamide gel electrophoresis for the separation of proteins in the range from 1 to 100 kDa. *Anal Biochem* **166:**368–379.

Strnad NP (1988) Binding of agonists and noncompetitive antagonists to the nicotinic acetylcholine receptor. Ph.D. Thesis, Washington University, St. Louis, MO.

Unwin N (1993) Nicotinic acetylcholine receptor at 9 A resolution. *J Mol Biol* **229:**1101–1124.

Unwin N (1995) Acetylcholine receptor channel imaged in the open state. *Nature (Lond)* **373:**37–43.

White BH, Howard S, Cohen SG and Cohen JB (1991) The hydrophobic photoreagent 3-(trifluoromethyl)-3-(M-[^{125}I]iodophenyl)diazirine is a novel noncompetitive antagonist of the nicotinic acetylcholine receptor. *J Biol Chem* **266:**21595–21607.

White BH and Cohen JB (1992) Agonist-induced changes in the structure of the acetylcholine receptor M2 regions revealed by photoincorporation of an uncharged nicotinic non-competitive antagonist. *J Biol Chem* **267:**15770–15783.

Wu G, Raines DE and Miller KW (1994) A hydrophobic inhibitor of the nicotinic acetylcholine receptor acts on the resting state. *Biochemistry* **33:**15375–15381.

Send reprint requests to: Dr. Jonathan B. Cohen, Department of Neurobiology, Harvard Medical School, 220 Longwood Ave., Boston, MA 02115. E-mail: jonathan_cohen@hms.harvard.edu